CCIT Report #403
November 2002

Image Sharpening by Flows Based on Triple Well Potentials

Guy Gilboa, Yehoshua Y. Zeevi
Department of Electrical Engineering,
Technion - Israel Institute of Technology,
Technion City, Haifa 32000, Israel

Nir Sochen
Department of Applied Mathematics,
University of Tel-Aviv
Ramat-Aviv, Tel-Aviv 69978, Israel

November 21, 2002

Abstract

Image sharpening in the presence of noise is formulated as a non-convex variational problem. The energy functional incorporates a gradient-dependent potential, a convex fidelity criterion and a high order convex regularizing term. The first term attains local minima at zero and some high gradient magnitude, thus forming a triple well-shaped potential (in the one-dimensional case). The energy minimization flow results in sharpening of the dominant edges, while most noisy fluctuations are filtered out.

Keywords: *image filtering, image enhancement, image sharpening, nonlinear diffusion, hyper-diffusion, variational image processing.*

1 Introduction

We address the issue of sharpening images degraded by blur-type operations and contaminated by additive noise. The approach is based on an evolutionary sharpening process, where in our case is derived from an energy minimization flow of a multi well-shaped energy density function. Somewhat similar type of flows where examined in the analysis of formation of microstructures in crystals [2, 10].

Let us first review the relation between nonlinear diffusion processes and energy minimization flows. We define a potential function (energy density) $\Psi(|\nabla I|)$ and a corresponding energy functional

$$E(I) = \int_{\Omega} \Psi(|\nabla I|) dx. \tag{1}$$

Minimization of this functional, using a gradient descent method, leads to a nonlinear diffusion process:

$$I_t = \mathrm{div}(J(\nabla I)) = \mathrm{div}(c(|\nabla I|^2)\nabla I), \tag{2}$$

where $J(\cdot)$ is the flux function given by

$$J(\nabla I) \doteq c(\cdot)\nabla I = \Psi'(|\nabla I|), \tag{3}$$

and $c(\cdot)$ is the diffusion coefficient. The initial condition is $I|_{t=0} = I_0$, where I_0 is in image processing applications the input image. Note that Neumann boundary conditions are assumed. (For more details see [9, 34, 30] and the references therein.)

Typical monotonically-increasing denoising potentials attain their minimum at zero. These type of potentials can be divided into two main groups: convex potentials (e.g. linear diffusion, Charbonnier et al. [6], Beltrami diffusion [28]) and nonconvex potentials (e.g. Perona-Malik [22]). Processes derived from convex potentials are well-posed, and their evolution approaches the minimum global energy (zero gradient magnitude everywhere, that is a constant function). Nonconvex potentials retain sturdier edge-preserving properties, their flux is not monotonic and the theory of the proper energy minimization process is more complex. Höllig [12] showed the existence of an infinite number of solutions to a diffusion process with nonmonotonic flux (non-convex potential) in one dimension. Yuo et al. [34] analyzed two-dimensional nonlinear diffusion and proved that processes based on a nonmonotone flux, with the condition

$$J(|\nabla I| \to \mathrm{inf}) = 0, \tag{4}$$

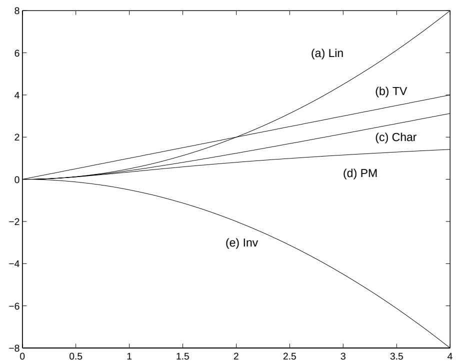

Figure 1: Potentials $\Psi(s)$ plotted as a function of the gradient magnitude s of some classical processes: (a) Linear forward diffusion ($\Psi = \frac{1}{2}s^2$), (b) TV ($\Psi = s$), (c) Charbonnier et al. ($\Psi = \sqrt{k^4 + k^2 s^2} - k^2$, $k = 1$), (d) Perona-Malik ($\Psi = \frac{1}{2}k^2 \log(1 + (\frac{s}{k})^2)$, $k = 1$), (e) Linear inverse (backward) diffusion ($\Psi = -\frac{1}{2}s^2$).

can have an infinite number of stationary points of the energy functional (and therefore are ill-posed). Both studies were restricted to the case of positive diffusion coefficients. Fortunately, it was discovered that regularizing the process by convolving the gradient with a Gaussian [5], or even by simple discretization [32], causes the the evolution to converge onto a constant trivial steady state unique solution. The only apparent instabilities are the staircasing effects [32, 30].

A limiting case between these two groups is the TV norm which has a non-strictly convex potential. To avoid numerical problems at low gradients, a small constant is usually added in the calculation of the gradient magnitude (i.e $|\nabla I|$ is substituted by $\sqrt{|\nabla I|^2 + \epsilon^2}$), turning the process into a convex one. (See Figs. 1,2 for examples of potential of some classical processes and of the corresponding diffusion coefficients.)

In cases of monotonically increasing potentials, the diffusion coefficients are positive. Thus the minimum-maximum principal is satisfied (the minimum and maximum of $I(t)$ is bounded by that of the initial condition I_0, for all $t > 0$ in any dimension) and no real sharpening can occur. Note that this is not the case for numerical schemes of systems with co-dimension > 1[7]. A classical ill-posed sharpening diffusion process is the linear backward (inverse) diffusion, where $c = const < 0$ and, consequently, the potential is

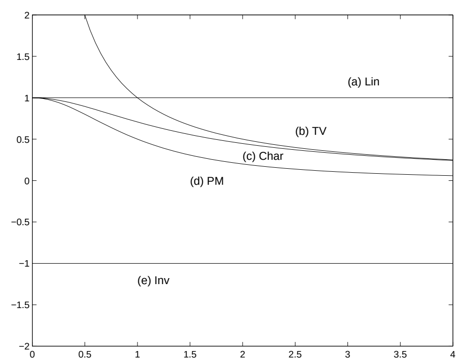

Figure 2: Diffusion coefficients $c(s)$ plotted as a function of the gradient magnitude s of the above processes: (a) Linear forward diffusion ($c = 1$), (b) TV ($c = \frac{1}{s}$), (c) Charbonnier et al. ($c = \frac{1}{\sqrt{1+s^2/k^2}}$, $k = 1$), (d) Perona-Malik ($c = \frac{1}{1+s^2/k^2}$, $k = 1$), (e) Linear inverse (backward) diffusion ($c = -1$).

strictly concave. This process attains its minimum energy at infinite gradient magnitudes, causing the explosion of the signal and severe noise amplification. We propose a nonconvex non-monotonic potential that overcomes most of the inverse diffusion instabilities, and yet is still powerful enough to sharpen, and increase contrast of, important features. We address some issues of regularization, and illustrate by numerical examples in one and two dimensions how this process is being implemented. This extends our previous study ([11]), where we proposed a forward-and-backward (FAB) diffusion process that shifts between denoising and sharpening, according to the local gradient features. In [26] the authors presented another study involving nonconvex potential using multiple wells. Their work is fundamentally different from ours since their potential is based on the signal and not its gradient, and its purpose is image classification. In [15] some interesting bounds on the norm of the solution to a gradient dependent inverse-diffusion problem in one dimension are given. The diffusion coefficient, though, is negative for small gradient magnitudes and the solution, tends, therefore, to create microstructures.

2 The Double Well Potential

Well-shaped potentials have been investigated recently in material science and structural mechanics [10, 2, 17]. In this section we review some of the mathematical and numerical aspects that are relevant to our case.

A mathematical model for the formation of microstructures in certain alloys was presented by Ball and James [2]. The theory is based on an energy minimization process of a double-well potential. The gradient-dependent potential attains its minimum value at symmetry-related deformation gradients [10, 2, 17]. In the one-dimensional case, a typical example of such potential is

$$\Psi(I_x) = (I_x^2 - k^2)^2. \tag{5}$$

Though it was not referred to as a diffusion process, and the outcome of this energy minimization flow does not resemble classical diffusion, it clearly can be viewed as a nonlinear diffusion process, with the following diffusion coefficient:

$$c(|I_x|) = 4(I_x^2 - k^2). \tag{6}$$

Plots of the potential and of the corresponding diffusion coefficient are provided in Fig. 3. This process is of a FAB type, where for low gradients $|I_x| < k$ it is a backward diffusion process, and for large gradients $|I_x| > k$ it is a forward one. This leads to the sharpening of low gradients and the smoothing of large gradients where both approach a magnitude of k ($I_x = \pm k$).

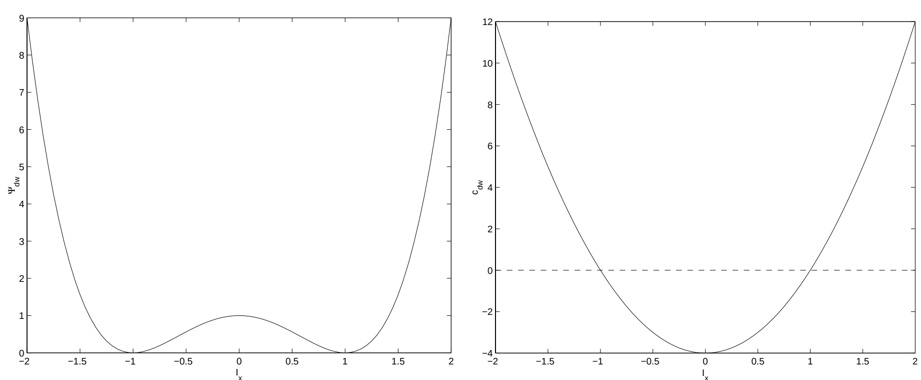

Figure 3: A double well potential (left) and the corresponding diffusion coefficient (right).

As the potential is non-convex and in some parts decreasing (creating an inverse diffusion flow), this process has stimulated a growing number of studies dealing with both the theoretical and numerical difficulties that it entails. (See for example [2, 4, 13, 17, 18, 20]).

Three main methods for numerical solutions of such problems were proposed [13]:

- Convexification of the potential, wherein the original potential is replaced by its convex hull. There exists a minimizer and it can be easily obtained, but at a cost of changing some of the process characteristics.
- Reformulation of the problem using Young measures (a mathematical tool in the calculus of variations applying a gradient-generated family of probability measures) [8, 21, 25].
- Direct minimization of the energy functional. In this type of methods, the process may converge onto a fixed point of a local minimum, because of the nonconvex nature of the problem. In some applications, though, those minima are also of interest.

The nature of the double-well and other related problems is quite similar to the formalism of our problem, and numerical techniques in image processing can most likely benefit from the research conducted in the (mathematically and computationally) related field. Yet, we should not overlook, and even stress, the following differences from the problem that we have at hand:

- The potential does not have a "relaxed" region, where gradients are being smoothed. Specifically, constant functions are unstable.
- The basic solution of the crystalline microstructure intends to have oscillations, which is not desirable in our case.
- The boundary conditions are different (Dirichlet versus Neumann in our case).
- The motivation is different: We are interested in the evolution of the input image, whereas analysis of the double-well model focuses on the final minimal energy state with weak relations to any primary initial evolutionary state.

3 Energy wells in image processing

3.1 The model

We assume the following general model of our degraded image Y:

$$Y = B(X) + n, \tag{7}$$

where X is the original image, B is a smoothing (blurring) transformation, not necessarily linear or shift invariant and n is some noise, uncorrelated with the signal (not necessarily white, but not of impulsive nature). We assume that large gradients (i.e. edges) of X are still relatively large in $B(X)$. After some sort of smoothing (or discretization) of Y (e.g. $\tilde{Y} = Y * g_\sigma = B(X) * g_\sigma + n * g_\sigma$) we assume that the gradient magnitude of the noise is less than an upper bound k with a very high probability (e.g. $\text{Prob}(|\nabla n * g_\sigma| < k) \to 1$).

Our objective is to sharpen important edges of the image. That is, edges with a relative large gradient magnitude in a neighborhood and with sufficient support. An imperative requirement is that noise should not be amplified in the process (and preferably even reduced). The noise amplification byproduct is a major drawback of many classical sharpening processes.

3.2 The Energy Functional

We choose to minimize the following energy functional:

$$E(I) = \int_\Omega (W(|\nabla I|) + \lambda F(I) + \varepsilon R(|\nabla^2 I|))dx, \tag{8}$$

where W is a potential generating a selective sharpening flow, F is a convex fidelity criterion related to the input image

$$F(I) = \rho(|I - I_0|). \tag{9}$$

We choose here $\rho(s) = \frac{1}{2}s^2$ but other choices are possible (e.g. [19]), and R is a higher order regularizing term (discussed later).

3.3 The Triple Well Potential

We begin by discussing the shape of the potential W derived from our objectives. The blurring process smears edges, thus gradients of large magnitude decrease. We would like to reverse this process and increase medium gradients back to their original state. Therefore high gradients should retain a lower energy state ("cost less energy") and the energy minimization process would thus be rewarded on edge sharpening.

However, two restrictions must be made: a saturation of the sharpening should be defined so very high gradients would not continue to be sharpened and cause the explosion of the signal. As we do not want to fall in the category of the ill-posed problems of condition (4), very large gradients should be even smoothed slowly, to reduce staircasing.

Secondly, low gradients should not be enhanced in order to avoid as much as possible noise amplification. Specifically, the zero gradient should not contribute any energy (be of zero potential).

From this discussion it follows that a potential intended for sharpening should be constructed of three basic attractors (low energy states) in one dimension: Two for high gradients (of positive and negative values) and one for the zero gradient. In two dimensions the potential is rotationally symmetric. This leads to a triple well-shaped potential.

Formally we set the following requirements:

$$\begin{array}{ll} (a) & W(0) = 0 \\ (b) & W(-s) = W(s), \quad \forall s \\ (c) & W(s) \geq 0, \quad \forall s \\ (d) & \exists\, 0 < a < b < \infty : W'(s \in (a,b)) < 0 \\ (e) & W'(s \to \infty) > 0. \end{array} \tag{10}$$

We suggest the following formula for the potential:

$$W(s) = \sqrt{k_f^4 + k_f^2 s^2} - k_f^2 - \frac{\alpha}{2} k_b^2 \log(1 + (\frac{s}{k_b})^2), \tag{11}$$

where k_f, k_b are parameters determining the lower-gradients *forward* diffusion region and the higher-gradients *backward* diffusion region, respectively ($k_f < k_b$), and α is a weight parameter. In order to fulfill (10.c) a proper bound on α should be set.

The corresponding diffusion coefficient is

$$c_W(s) = \frac{1}{\sqrt{1 + (s/k_f)^2}} - \frac{\alpha}{1 + (s/k_b)^2}. \tag{12}$$

The potential is 'designed' such that the resultant diffusion coefficient is as simple as possible; After all, we use the diffusion coefficient to compute the

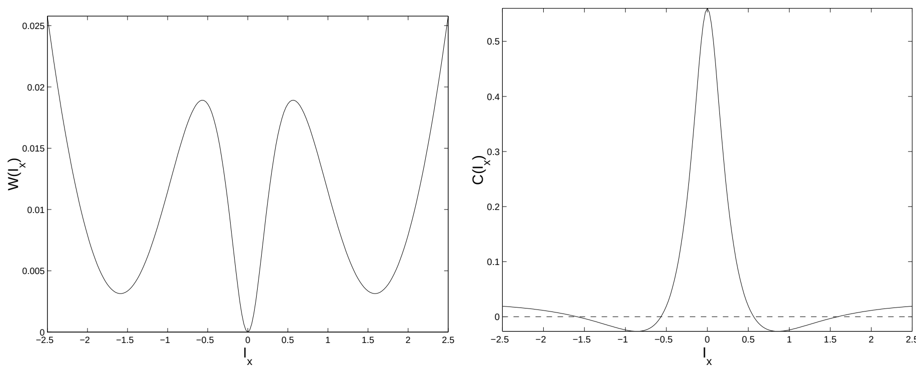

Figure 4: A triple well potential (left) and the corresponding one-dimensional diffusion coefficient (right).

flow in the numerical implementation. (See Fig. 4 for plots of W and c_W.) Other, more sophisticated formulas, with more parameters controlling the shape of the potential, can be used. In [11] we proposed a different formula for a forward-backward diffusion coefficient. However, in that study the process was not formulated as a variational problem. As a consequence some of the stabilizing elements introduced here where not included in the earlier study, namely, the restriction to positive potentials, the positive diffusivity at very large gradients and the addition of higher order regularization.

3.4 Higher Order Regularization

We wish to have the 'smoothest' possible energy minimizer in order to reduce oscillations between the three low energy states. (The reasoning is similar to what is given in cases of viscosity solutions). For this purpose we add the following high order convex regularization term to the total energy density function:

$$R(|\nabla^2 I|) = \frac{1}{2}|\nabla^2 I|^2. \tag{13}$$

This adds a linear fourth order term $-\nabla^4 I$ to the gradient descent flow, where ∇^4 is the *biharmonic operator* (or *bi-Laplacian*). In the one-dimensional case, $\nabla^4 I = I_{xxxx}$, whereas in two dimensions $\nabla^4 I = I_{xxxx} + 2I_{xxyy} + I_{yyyy}$. The fourth order linear equation

$$I_t = -\nabla^4 I, \quad I|_{t=0} = I_0 \tag{14}$$

is often referred to as a hyper-diffusion flow (also super-diffusion). The fundamental solution of (14) in the frequency domain of (ω) is $e^{-\omega^4 t}$, implying that it is a strongly-low-pass filtering flow that rapidly diminishes high frequency oscillations. (See Fig.5 for plots of the fundamental solution, and Figs. 6, 7 for examples of hyper-diffusion in one and two dimensions.) A nonlinear hyper-diffusion term was added in [29] to the standard Perona-Malik equation [22], to rapidly remove the noise. Note, though, that hyper-diffusion does not obey the minimum-maximum principle (the spatial fundamental solution is not strictly positive and resembles more the the ideal lowpass *sinc* function (Fig. 5)). Thus, its implementation for denoising purposes should be executed with care.

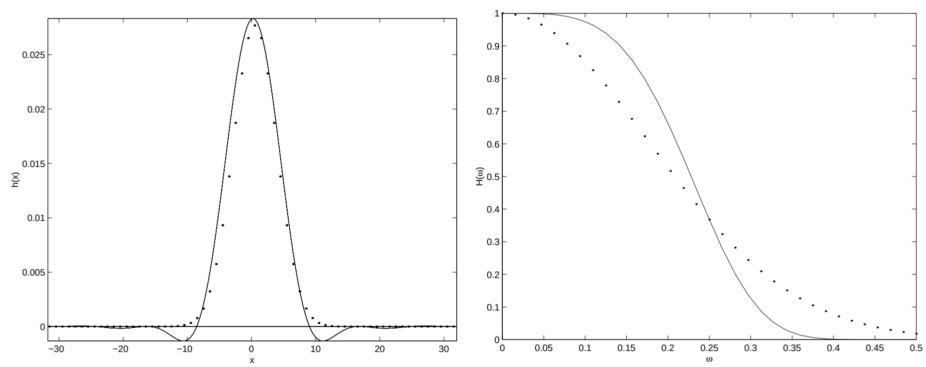

Figure 5: Fundamental solution of the hyper-diffusion (line) vs. diffusion (dots), plotted in the spatial domain (left) and frequency domains (right). Whereas the diffusion kernel is a Gaussian in both domains, the hyper-diffusion has a sharper frequency cutoff and is not strictly positive in the spatial domain.

The Cahn-Hilliard [3] and Kuramoto-Sivashinsky [14, 27] equations have a hyper-diffusion term, that is stabilizing inverse diffusion processes (along with a first order nonlinearity). These equations were used to model evolution of phase fields in alloy mixtures [3], oscillatory chemical reactions [14] and fronts of premixed flames [27], among other natural phenomenon [24, 33].

It was shown in [33] that a nonlinear forward-backward diffusion process with higher order regularization (of hyper-diffusion and a viscous relaxation term) yields a unique solution. Although the equations are different (e.g. the nonlinear diffusion coefficient in [33] is a function of the signal itself $(c = c(I))$

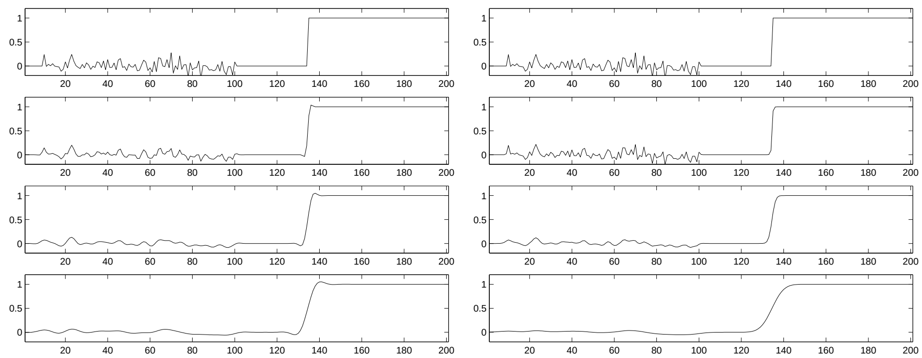

Figure 6: Comparison of hyper-diffusion (left) and linear diffusion (right) processing of noise and a step edge, given at times 0, 0.1, 1, 10 (from top to bottom, respectively). Hyper-diffusion diminishes high frequency noise more rapidly, while low frequencies decay slower. Also, hyper-diffusion does not obey the minimum-maximum principle (most apparent in the step processing).

and not of its gradient), we assume that similar results can be obtained in our case.

Figure 7: Hyper-diffusion processing of the cameraman image, given at normalized times 0 (top-left), 0.1 (top-right), 1 (bottom-left), 10.

3.5 Energy Minimization Flow

We use the following dissipating energy process:

$$\begin{aligned} &I_t = \operatorname{div}(c_W(|\nabla I|^2)\nabla I) + \lambda(I_0 - I) - \varepsilon \nabla^4 I, \\ &I|_{t=0} = I_0,\ \partial_n I|_{x\in\partial\Omega} = 0,\ \partial_n^2 I|_{x\in\partial\Omega} = 0, \end{aligned} \tag{15}$$

where n is a unit vector, normal to the boundary $\partial\Omega$. The second boundary condition is stated in this case for the fourth order PDE to be well defined (in addition to the standard first order Neumann BC).

4 Examples

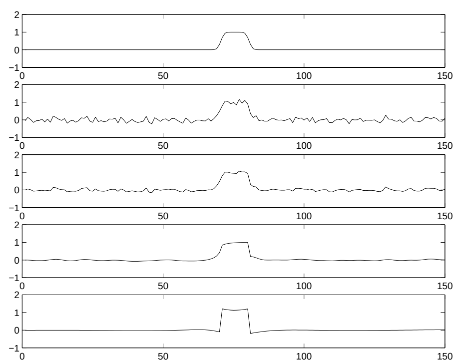

Figure 8: Straight edge with additive white Gaussian noise (SNR=7dB).

A one dimensional signal resembling a blurred line (two close step edges of opposite signs), with additive noise, was processed (Fig. 8. This example demonstrates a noise removing process sharpens edges. Whereas the two edges are sharpened, the noise was smoothed out. This process can handle multiple types of blurs, both isotropic and anisotropic, simultaneously (Fig. 9. This is in contrast to deconvolution techniques that assume either an *a priori* known or an unknown (blind deconvolution) stationary (generally linear) blurring kernel. In 10 a blurred flower image is processed. We used adaptive parameters (k_f, k_b) for the triple-well potential, as described in [11], to be able to sharpen a wide range of gradient edges. Though edges are sharper, there are still some staircasing effects and the edges are not so smooth. A

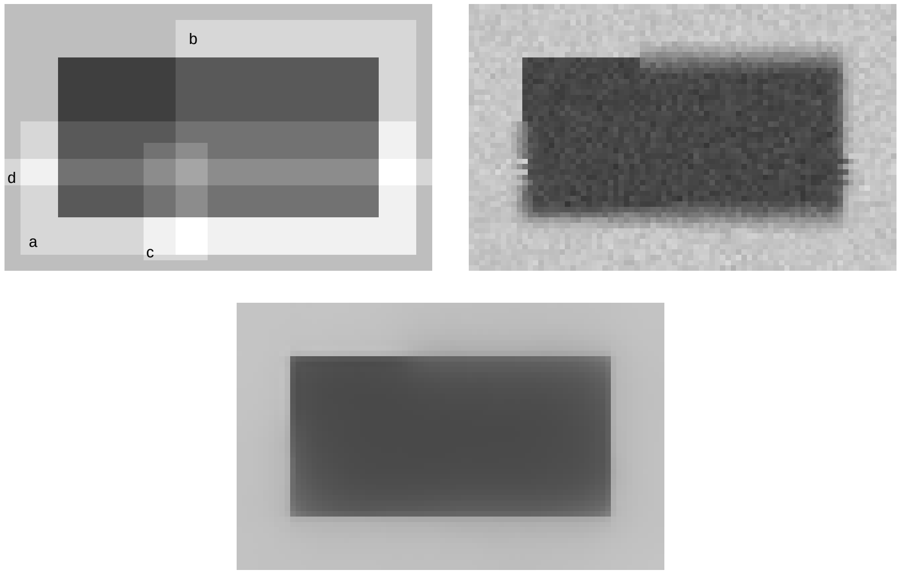

Figure 9: Processing of a non-stationarily blurred step image, contaminated by additive noise. Top left: Degradation function, highlighting regions of different types of degradations: (a) Isotropic Gaussian blur ($\sigma = 2$), (b) Anisotropic exponential blur, $e^{-|x|+|y|/5}$, (c) 5x5 uniform averaging blur, (d) Jagginess. Regions overlapped by a few filters were processed by all of them. Top right - degraded image, with added Gaussian white and uniform white noise (SNR=15dB). Bottom - processed image.

straightforward improvement could be the implementation of tensor diffusivity, instead of a scalar one (as in Weickert's coherence enhancing diffusion [31]), where the sharpening triple-well potential is used across the edge, and some smoothing potential is used along the edge.

The numerical implementation consists of two iterative stages: at each time step, the nonlinear FAB diffusion, with a fidelity term, is calculated by a standard 3x3 template. The second stage implements the linear hyper-diffusion, by convolution with a 5x5 kernel (the minimal support required in the case of a fourth order equation). For the triple-well potential we used, in all examples, $\alpha = 2.2k_f/k_b$.

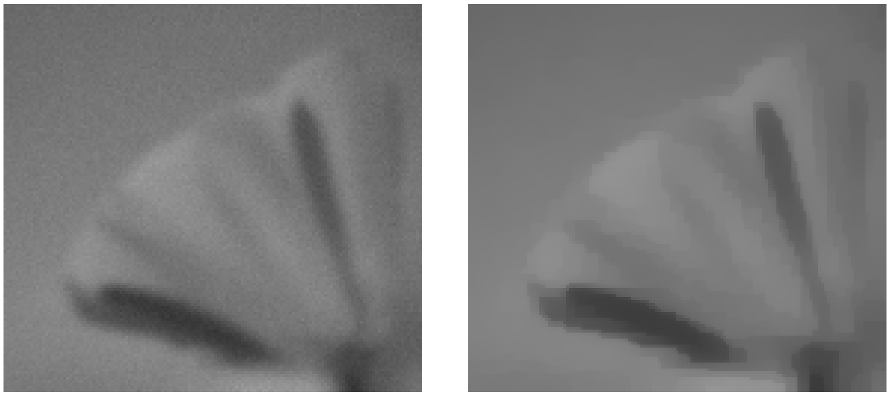

Figure 10: Processing of a Gaussianly blurred flower image, ($\sigma = 2$), contaminated by white Gaussian noise (SNR=15dB). Left - input image, right - processed image.

5 Discussion and Conclusion

The main novelty of this study is the formulation of sharpening processes according to a variational framework. The task has been to increase important gradients (edges), in order to reverse the blurring effect, required to be accomplished without noise amplification and by avoiding signal 'explosion'. These aims and constraints led us to propose a gradient dependent functional in the form of a triple-well. The process is a FAB diffusion-type, sharpening sharp edges while denoising fluctuations and noise.

To accomplish the desired task, two additional terms were added to the general energy functional: a standard fidelity term and the square magnitude of the Laplacian, serving as a high order regularizing term. The energy minimization of the last term leads to a hyper-diffusion flow; a fourth order process that entails strong low-pass filtering, and can attenuate high frequency oscillations that are characteristic of inverse diffusion. The hyper-diffusion eliminates the effect of enhancement of isolated points, otherwise sharpened by the triple-well potential. Moreover, edges become more coherent. As the weight of this smoothing term increases, the sharpening affects become less apparent. Some other affects of hyper-diffusion on the general process are yet to be fully analyzed and understood. Also, effort should be directed to reach conclusions regarding stability properties and well-posedness of the equations.

The use of triple-well potentials could be generalized to color images, using the Beltrami framework, and may be extended to other processes intended for feature sharpening.

Acknowledgments

We thank Philip Rosenau for interesting discussions. This research has been supported in part by the Ollendorf Minerva Center, the Fund for the Promotion of Research at the Technion, Israel Academy of Science, Tel-Aviv University fund, the Adams Center and the Israeli Ministry of Science. YYZ is presently supported also by the Medical imaging Group of the Department of BME, Columbia University, and by the ONR MURI Program N000M-01-1-0625.

References

[1] L. Alvarez, L. Mazorra, "Signal and image restoration using shock filters and anisotropic diffusion", SIAM J. Numer. Anal. Vol. 31, No. 2, pp. 590-605, 1994.

[2] J. Ball, R. James, "Proposed experimental tests of a theory of fine microstructure and the two-well problem", Phil. Trans. R. Soc. Lond. A, 338:389-450, 1992.

[3] J.W. Cahn, J.E. Hilliard, "Free Energy of a Nonuniform System. I. Interfacial Free Energy", J. Chem. Phys. 28,2 258-267, 1958.

[4] C. Carstensen, P. Plechac, "Adaptive mesh refinement in scalar nonconvex variational problems", Berichtsreihe des Mathematischen Seminars Kiel 97-2, 1997.

[5] F. Catte, P. L. Lions, J. M. Morel and T. Coll, "Image selective smoothing and edge detection by nonlinear diffusion", SIAM J. Num. Anal., vol. 29, no. 1, pp. 182-193, 1992.

[6] P. Charbonnier, L. Blanc-Feraud, G. Aubert, M. Barlaud, "Two deterministic half-quadratic regularization algorithms for computed imaging", Proc. IEEE ICIP '94, Vol.2, 168-172, 1994.

[7] L. Dascal, N. Sochen, to appear.

[8] S. Demoulini, "Young measure solutions for a nonlinear parabolic equation of forward-backward type", SIAM J. Math. Anal., 27(1996), pp. 376-403.

[9] R. Deriche, O. Faugeras, "Les EDP en traitement des images et vision par ordinateur", Technical report, INRIA, November 1995.

[10] J. Ericksen, "Some constrained elastic crystals", in John Ball, editor, Material Instabilities in Continuum Mechanics and Related Problems, pp. 119-137, Oxford, 1987, Oxford Univ. Press.

[11] G. Gilboa, N. Sochen, Y.Y. Zeevi, "A Forward-and-Backward Diffusion Process for Adaptive Image Enhancement and Denoising", IEEE Transactions on Image Processing, Vol. 11, No. 7, pp. 689-703, July 2002.

[12] K. Höllig, "Existence of infinitely many solutions for a forward-backward heat equation", Trans. Amer. Math. Soc. 278, 299-316, 1983.

[13] M.K. Gobbert, A. Prohl, "A Survey of Classical and New Finite Element Methods for the Computation of Crystalline Microstructure", IMA preprints, 1576, June 1998.

[14] Y. Kuramoto, *Chemical Oscillations, Waves, and Turbulence*, Springer-Verlag, New York, 1984.

[15] A. Kurganov, Doron Levy, Philip Rosenau, "On Burgers-type Equations with Non-monotonic Dissipative Fluxes", Communications on Pure and Applied Mathematics 51 (1998), 443-473.

[16] M. Kerckhove (Ed.), "Scale-Space and morphology in computer-vision", Scale-Space 2001, LNCS 2106, Springer-Verlag 2001.

[17] M. Luskin, "Approximation of a laminated microstructure for a rotationally invariant, double well energy density", Numer. Math., 75 : 1997, 205-221.

[18] J. Munoz, P. Pedregal, "Explicit solutions of nonconvex variational problems in dimension one", Applied Math.and Optimization, 41(1), 129-140, 2000.

[19] M. Nikolova, "Minimizers of cost-functions involving non-smooth data-fidelity terms. Application to the processing of outliers", to appear in SIAM Journ. on Numerical Analysis.

[20] P. Pedregal, "On the numerical analysis of non-convex variational problems", Numer. Math. 1996 74(03) P 325.

[21] P. Pedregal, "Optimization, relaxation and Young measures", Bull. Amer. Math. Soc. 36 (1999), 27-58.

[22] P. Perona and J. Malik, "Scale-space and edge detection using anisotropic diffusion", IEEE Trans. Pat. Anal. Machine Intel., 12(7):629-639, 1990.

[23] B M ter Haar Romeny Ed., *Geometry Driven Diffusion in Computer Vision*, Kluwer Academic Publishers, 1994.

[24] M. Rost, J. Krug, "A practical model for the Kuramoto-Sivashinsky equation", Physica D 88, 1-13, 1995.

[25] T. Roubicek, *Relaxation in Optimization Theory and Variational Calculus*, Walter de Gruyter, Berlin, New York, 1997.

[26] C. Samson, L. Blanc-F?raud, G. Aubert, J. Zerubia, "A variational model for image classification and restoration", IEEE Trans. Pat. Anal. Machine Intel., 22(5):460-472, 2000.

[27] G.I. Sivashinsky, "Instabilities, Pattern Formation, and Turbulence in Flames", Ann. Rev. Fluid Mech., v. 15, pp. 179-199 (1983).

[28] N. Sochen, R. Kimmel, R. Malladi , "A general framework for low level vision", *IEEE Trans. on Image Processing*, 7, (1998) 310-318.

[29] G.W. Wei, "Generalized Perona-Malik equation for Image Restoration", IEEE Signal Processing Lett. , 6 , pp. 165-167 (1999).

[30] J. Weickert, "A review of nonlinear diffusion filtering", B. ter Haar Romeny, L. Florack, J. Koenderink, M. Viergever (Eds.), Scale-Space Theory in Computer Vision, LNCS 1252, Springer, Berlin, pp. 3-28, 1997.

[31] J. Weickert, "Coherence-enhancing diffusion filtering", International Journal of Computer Vision, Vol. 31, 111-127, 1999.

[32] J. Weickert, B. Benhamouda, "A semidiscrete nonlinear scale-space theory and its relation to the Perona-Malik paradox", F. Solina (Ed.), Advances in computer vision, Springer, Wien, 1-10, 1997

[33] Thomas P Witelski, "The structure of internal layers for unstable nonlinear diffuison equations", Studies in Applied Mathematics, 96, pp. 277-300, (1996).

[34] Y. Yuo, W. Xu, A. Tannenbaum, M. Kaveh, "Behavioral analysis of anisotropic diffusion in image processing", IEEE Trans. Image Process, Vol. 5, No. 11, 1996.